Subharmonic structure of Shapiro steps in frustrated superconducting arrays

Seunghwan Kim,* Beom Jun Kim, and M. Y. Choi
Department of Physics and Center for Theoretical Physics, Seoul National University, Seoul 151-742, Korea
(Received 29 March 1995; revised manuscript received 20 June 1995)

Two-dimensional superconducting arrays with combined direct and alternating applied currents are studied both analytically and numerically. In particular, we investigate in detail current-voltage characteristics of a square array with $\frac{1}{2}$ flux quantum per plaquette and triangular arrays with $\frac{1}{2}$ and $\frac{1}{4}$ flux quantum per plaquette. At zero temperature reduced equations of motion are obtained through the use of the translational symmetry present in the systems. The reduced equations lead to a series of subharmonic steps in addition to the standard integer and fractional giant Shapiro steps, producing devil's staircase structure. This devil's staircase structure reflects the existence of dynamically generated states in addition to the states originating from degenerate ground states in equilibrium. Widths of the subharmonic steps as functions of the amplitudes of alternating currents display Bessel-function-type behavior. We also present results of extensive numerical simulations, which indeed reveal the subharmonic steps together with their stability against small thermal fluctuations. Implications for topological invariance are also discussed.

I. INTRODUCTION

In the past several years there have been extensive studies on two-dimensional (2D) $N\times N$ arrays of superconductors, weakly coupled by Josephson junctions, because of their interesting phase transitions and dynamical behaviors.[1] While the initial studies on these systems were devoted to investigate mostly equilibrium properties, more recently growing interest has centered about their dynamical properties in the presence of external currents. In this case the system is known to display characteristic current-voltage (IV) relations, such as the universal jump in the exponent of the relation under applied direct currents[2] and quantized voltage plateaus, called giant Shapiro steps, in the presence of combined direct and alternating currents.[3] In particular, in the presence of an external magnetic field corresponding to $f=p/q$ flux quanta per plaquette, plateaus are found to occur at voltages $(n/q)N\hbar\omega/2e$, where n is an integer and ω is the frequency of the applied current. These fractional as well as integer steps were interpreted as resulting from coherent oscillations of the ground-state configurations of field-induced vortices, and successfully reproduced in numerical simulations performed on arrays of resistively shunted junctions (RSJ's).[3] Analytical confirmation of these results is rather difficult due to the nonlinear nature of the coupled equations of motion for the system, and there have been proposed some qualitative arguments trying to explain the quantization in terms of the vortex motion[3,4] and of topological invariance.[5]

In addition to these integer and fractional giant Shapiro steps, the appearance of subharmonic Shapiro steps was reported in arrays of overdamped junctions,[3,4] which has been a source of controversy since a single overdamped junction (with negligible capacitance) is well known not to display such subharmonic steps. In simulations, on the other hand, subharmonic steps were found to occur only when free transverse boundary conditions were employed; with periodic boundary conditions, such structure did not appear,[3] suggesting that the subharmonic steps were merely finite-size effects. Although subharmonic steps were also predicted in arrays with diagonally injected bias currents,[6] numerical simulations as well as experiments ruled out such a possibility.[7] Thus the subharmonic steps, experimentally observed only in arrays with usual in-line current injection, have been proposed to originate from the self-induced magnetic fields.[4] Subsequent theoretical analysis of arrays with finite inductance indeed has given results in support of such interpretation.[8] The existence of such subharmonic steps in general reflects that the equation of motion cannot be reduced to a single (first-order) differential equation, and is presumably generic in a system governed by a few coupled equations (instead of a single equation), including the frustrated systems, i.e., arrays in external magnetic fields. A recent analytical and numerical study of a fully frustrated ($f=1/2$) array of RSJ's indeed revealed the possibility of a subharmonic structure *in the absence of inductance*. Further, evidence for steps at every rational value of voltages, which is suggestive of a devil's staircase structure, has been reported.[9,10]

This paper investigates in detail the responses of 2D arrays of Josephson junctions to combined direct and alternating currents, with regard to the possibility of the subharmonic structure of Shapiro steps in the absence of both capacitance and inductance. We consider square and triangular arrays of RSJ's whose time evolutions are governed by sets of coupled Langevin equations. At zero temperature the translational symmetry in the systems allows us to reduce the corresponding equations of motion to a few coupled equations, from which current-voltage characteristics can be calculated. Remarkably, we find a series of subharmonic steps in addition to the standard integer and fractional steps, which strongly suggests a devil's staircase structure. Such structure is formed out of dynamically accessible states: Some of them are generated dynamically while others originate from degenerate ground states in equilibrium. Widths of subharmonic steps are calculated for various amplitudes of alternating currents, and found to display Bessel-function-type

0163-1829/95/52(18)/13536(11)/$06.00

behavior. Extensive numerical simulations indeed reveal the subharmonic steps together with stability against small thermal fluctuations.

There are six sections in this paper: Section II introduces the $N\times N$ array of RSJ's with usual in-line current injection, and describes the set of N^2 coupled Langevin equations which specifies the time evolution of the system. In Sec. III we consider a fully frustrated square array, for which the equations of motion are reduced to two coupled equations. This allows us to calculate the IV characteristic, which exhibits a series of subharmonic steps. The time evolution is shown to be described by four dynamically accessible states, two of which correspond to the doubly degenerate ground states. Sections IV and V are devoted to the IV characteristics of triangular arrays, with $f=1/2$ and $f=1/4$, respectively. Subharmonic structures similar to that in the square array are again found, and results of numerical simulations confirming such subharmonic steps are presented. Finally, a brief summary is given in Sec. VI.

II. ARRAYS DRIVEN BY EXTERNAL CURRENTS

We consider an $N\times N$ array of resistively shunted junctions in the presence of a uniform transverse magnetic field. We take periodic boundary conditions along the direction perpendicular to the external current and free boundary conditions along the longitudinal direction. Thus along one edge of the array ($y=0$) a combined direct and alternating current $I=I_{\rm dc}+I_{\rm ac}\sin\omega t$ is injected into each node, while along the opposite edge ($y=N$) the same current I is extracted from each node. Neglecting capacitive and inductive effects, we write the net current from grain i to grain j as the sum of a Josephson current, a normal current, and a thermal noise current:

$$I_{ij}=I_c\sin(\phi_i-\phi_j-A_{ij})+\frac{V_{ij}}{R}+L_{ij}, \tag{1}$$

where ϕ_i is the phase of the superconducting order parameter at site $i\equiv(x_i,y_i)$, I_c is the critical current of the junction, $V_{ij}\equiv V_i-V_j$ is the potential difference across the junction, and R is the shunt resistance. In the limit of the large penetration depth, the bond angle A_{ij} is given by the line integral of the vector potential $\mathbf{A}$ due to the external magnetic field:

$$A_{ij}=\frac{2\pi}{\Phi_0}\int_i^j \mathbf{A}\cdot d\mathbf{l}, \tag{2}$$

with the flux quantum $\Phi_0\equiv hc/2e$. The plaquette sum of A_{ij} is equal to $2\pi f$, where f is the uniform frustration given by the flux per plaquette in units of Φ_0. The thermal noise current L_{ij} at temperature T is assumed to satisfy

$$\langle L_{ij}(t+\tau)L_{kl}(t)\rangle=\frac{2k_BT}{R}\delta(\tau)(\delta_{ik}\delta_{jl}-\delta_{il}\delta_{jk}), \tag{3}$$

where $\langle\cdots\rangle$ denotes an ensemble average. Equation (3) is a generalization of the noise current used in the discussion of a single Josephson junction.[11]

The potential is related to the phase by the Josephson relation $d(\phi_i-\phi_j-A_{ij})/dt=2eV_{ij}/\hbar$. The current conservation at each site then allows us to write Eq. (1) in the form of a set of N^2 coupled equations:

$$I_i^{\rm ext}=\sum_j{}'\left[\frac{\hbar}{2eR}\frac{d}{dt}(\phi_i-\phi_j-A_{ij})+I_c\sin(\phi_i-\phi_j-A_{ij})+L_{ij}\right], \tag{4}$$

where $I_i^{\rm ext}$ is the external current fed into grain i, and the summation is over the nearest neighbors of i. In the model considered here, we have $I_i^{\rm ext}=I(\delta_{y_i,0}-\delta_{y_i,N})$. Introducing dimensionless parameters

$$I_i=\frac{I_i^{\rm ext}}{I_c},\quad \eta_{ij}=\left(\frac{\hbar I_c}{2ek_BT}\right)^{1/2}\frac{L_{ij}}{I_c}\equiv\frac{L_{ij}}{\gamma I_c}, \tag{5}$$

we write Eq. (4) in the dimensionless form,

$$\frac{d\phi_i}{dt}=\sum_j G_{ij}\left\{I_j-\sum_k{}'\left[\sin(\phi_j-\phi_k-A_{jk})+\gamma\eta_{jk}\right]\right\}, \tag{6}$$

where time t has been rescaled in units of $\hbar/2eRI_c$, G_{ij} is the lattice Green's function defined by $\Sigma_j'(\phi_i-\phi_j)=\Sigma_j G_{ij}^{-1}\phi_j$, and the noise η_{ij} is characterized by $\langle\eta_{ij}(t+\tau)\eta_{kl}(t)\rangle=2\delta(\tau)(\delta_{ik}\delta_{jl}-\delta_{il}\delta_{jk})$.

The set of Langevin equations (6) constitutes the equations of motion, which govern the time evolution of the system. When the array is driven by direct currents ($I_{\rm ac}=0$), it is convenient to consider the corresponding Fokker-Planck equation, the stationary solution of which leads to an effective Hamiltonian in the form of the washboard potential. Thus the phase transitions as well as the IV characteristics displayed by the effective Hamiltonian have been investigated.[12] In the case of driving with combined direct and alternating currents, on the other hand, the explicit time dependence in general prohibits the equilibrium description, making it necessary to consider the set of Langevin equations (6) directly. Obviously, however, the analytical investigation of the N^2 coupled nonlinear equations cannot be performed. We thus use the symmetry at zero temperature to reduce the number of equations to a few and integrate the reduced equations. To confirm the results obtained from the reduced equations, we also perform extensive numerical simulations directly of Eq. (6).

III. SQUARE ARRAY WITH $f=1/2$

We begin with a fully frustrated square array, with the frustration $f=1/2$.[9,13,14] Using the symmetry present in the ground state of the system, one can reduce Eq. (6) to two coupled equations for $\chi\equiv(\alpha+\gamma)/2$ and $\psi\equiv(\alpha-\gamma)/2$:

$$\frac{d\chi}{dt}=\frac{1}{2}(\cos\chi-\sin\chi\cos\psi),\quad \frac{d\psi}{dt}=I(t)-\cos\chi\sin\psi, \tag{7}$$

where we have followed Ref. 9 for the definitions of the gauge-invariant phase differences α, β, and γ. Equations (7) have been studied to give the standard integer and fractional giant Shapiro steps,[15] and further, detailed study with

high precision has revealed the fine structure: subharmonic steps at rational values of $\langle V \rangle$ in units of $N\hbar\omega/2e$. It exhibits not only subharmonic steps but also self-similarity, apparently producing the devil's staircase structure.[9]

In order to understand the nature of the subharmonic structure, we consider the time evolution of gauge-invariant phase differences α and γ, vortex charge $\Delta \equiv (\alpha + 2\beta + \gamma)/2\pi$ at a particular plaquette, potential difference V between the top and the bottom of the superlattice unit cell, and quasienergy $E_s \equiv (\cos\alpha + 2\cos\beta + \cos\gamma)/2$. Here the quasienergy E_s corresponds to the (equilibrium) energy in the absence of external currents, and α, β, and γ are defined in the interval $[-\pi, \pi)$.

We first consider integer and half-integer steps, and present in Fig. 1 the time evolution of α, γ, Δ, V, and E_s in the stationary state on $\langle V \rangle$ = (a) 1/2, (b) 1, (c) 3/2, and (d) 2. Figure 1(a) shows that α and γ are periodic in time with period 20 (again in units of $\hbar/2eRI_c$), which corresponds to $2(2\pi/\omega)$ since we have taken $\omega = \pi/5$ in the numerical integration of Eqs. (7). It also reveals that there exist two states characterized by vortex charge $\Delta = \pm 1/2$: $\Delta = 1/2$ during $1 \lesssim t \lesssim 11$ and $\Delta = -1/2$ during $11 \lesssim t \lesssim 21$. Typical configurations of these two states are $\mathscr{A}$ and $\mathscr{B}$ of Fig. 2, respectively, which are precisely the doubly degenerate ground states in equilibrium. It can also be observed that the system stays mostly in the states with the quasienergy $E_s = -\sqrt{2}$ which is just the ground state energy in equilibrium. While the system stays in either state, the potential difference fluctuates around zero, which implies that they are not voltage carrying states. It is thus concluded that the two states originate from the ground states in equilibrium. The change of the vortex charge from $+1/2$ to $-1/2$ (and vice versa) corresponds to the vortex motion from one ground state to the other, leading to the half-integer step. Figure 1(b) also displays the periodic evolution of the system with period $(2\pi/\omega)$, corresponding to the integer step $\langle V \rangle = 1$. The vortex charge Δ at the plaquette takes the value $-1/2$ only momentarily; it stays with the value 1/2 for the most time. Whereas the state $\Delta = 1/2$ has the typical configuration of $\mathscr{A}$, the state $\Delta = -1/2$ during $9.5 \lesssim t \lesssim 11.5$ does not correspond to the ground state. The quasienergy and the potential difference of this state are larger than those of states originating from the ground state, implying that the state is unstable and voltage carrying. This suggests that it should be interpreted as a transient state involved in the vortex motion. The typical configuration of such a transient state is shown in $\mathscr{C}$ of Fig. 2. It is also found that the system starting from other initial conditions may exhibit different time evolution; it spends most of the time in state $\Delta = -1/2$ with the typical configuration given by $\mathscr{B}$, and visits momentarily the state $\Delta = 1/2$ with the typical configuration of $\mathscr{D}$. These observations on integer and half-integer steps are consistent with the explanations in terms of the vortex motion[3,4] and of topological invariance.[5] In Fig. 1(c) we show the time evolution of α, γ, Δ, E_s, and V on the higher-order half-integer step $\langle V \rangle = 3/2$. Here α and γ are periodic with period $2(2\pi/\omega)$, which is the same as the period on $\langle V \rangle = 1/2$. However, there are voltage-carrying transient states involved, and the time evolution during one period $(12 \lesssim t \lesssim 32)$ follows the sequence $\{\mathscr{ACDBDC}\}$. Each

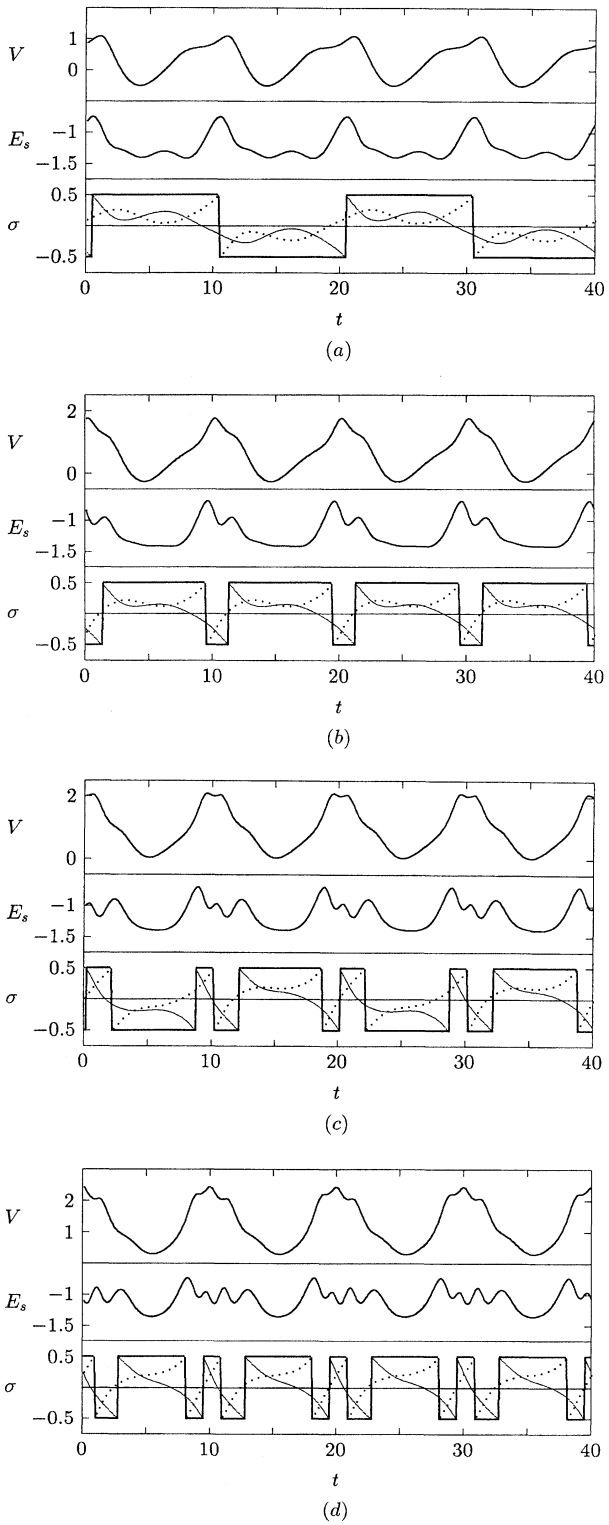

FIG. 1. Stationary-state time evolution of potential difference V, quasienergy E_s, phase differences α and γ, and vortex charge Δ in a square array with $f = 1/2$ on half-integer and integer steps, (a) $\langle V \rangle = 1/2$, (b) $\langle V \rangle = 1$, (c) $\langle V \rangle = 3/2$, and (d) $\langle V \rangle = 2$. σ represents α (dotted line), γ (thin line), or Δ (thick line).

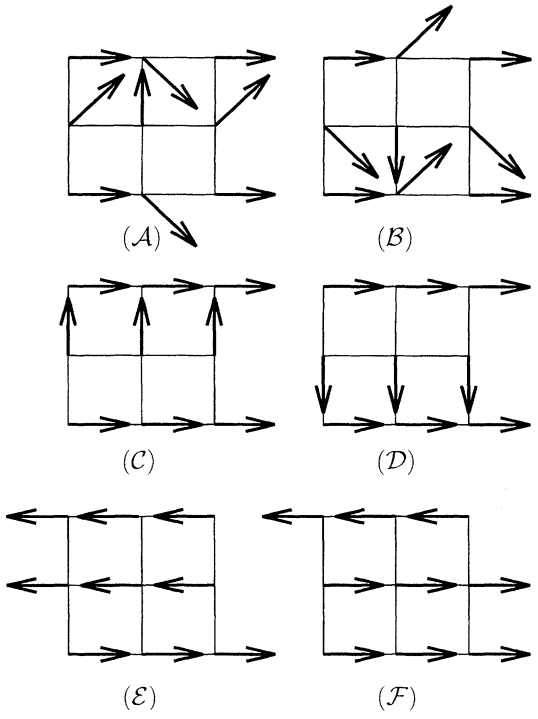

FIG. 2. Typical configurations of the states found in Figs. 1 and 3, with arrows denoting the phases. In the gauge chosen here, $A_{ij}=\pi$ for vertical bonds at the center of each diagram; for other bonds, $A_{ij}=0$. $\mathscr{A}$ and $\mathscr{B}$ are doubly degenerate ground states in equilibrium, while $\mathscr{C}$ and $\mathscr{D}$ are transient states. The phases in $\mathscr{E}$ and $\mathscr{F}$, which are dynamically generated states, are not periodic under translation by the vortex superlattice constant; however, the gauge-invariant phase differences are periodic.

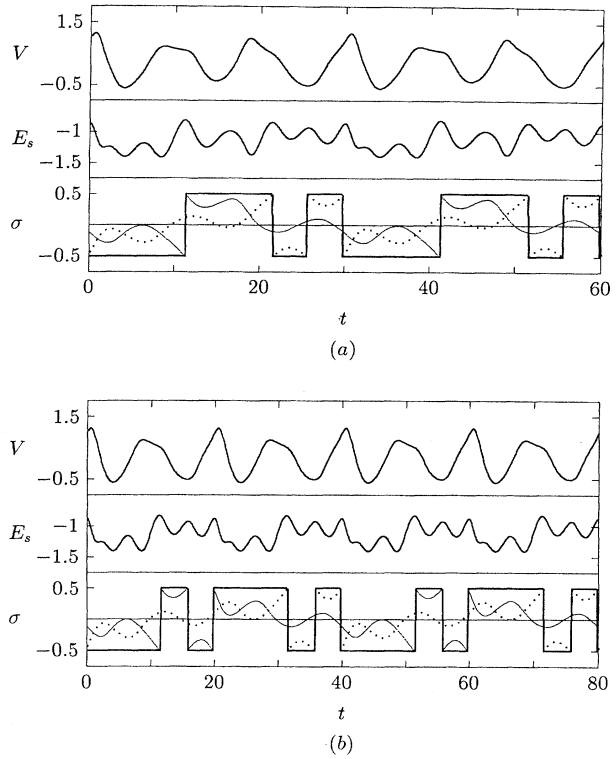

FIG. 3. Time evolution of α, γ, Δ, E_s, and V in a square array with $f=1/2$ on subharmonic steps, (a) $\langle V\rangle=1/3$ and (b) $\langle V\rangle=1/4$. σ again represents α (dotted line), γ (thin line), or Δ (thick line).

state can be identified easily from the time evolution of α, γ, and Δ. On the step $\langle V\rangle=5/2$ (not shown here), the period is also found to be $2(2\pi/\omega)$ with the time evolution $\{\mathscr{ACDCDBDCDC}\}$ during one period. Figure 1(d) exhibits the time evolution on the higher-order integer step $\langle V\rangle=2$, which reveals that the period is the same as that on $\langle V\rangle=1$, i.e., $(2\pi/\omega)$. Here more transient states intervene in the time evolution, which follows the sequence $\{\mathscr{ACDC}\}$ in one period. We have also investigated the step $\langle V\rangle=3$, and find that the period is again $(2\pi/\omega)$ together with the time evolution $\{\mathscr{BDCDCD}\}$.

We next examine the subharmonic steps $\langle V\rangle=1/q$ with $q>2$, and display in Fig. 3 the time evolution of α, γ, Δ, E_s, and V on $\langle V\rangle=$ (a) 1/3 and (b) 1/4. Figure 3(a) reveals that α and γ are periodic with period $3(2\pi/\omega)$, leading to $\langle V\rangle=1/3$, and that there appear three different states: Two of them (the states $\Delta=1/2$ during $11\lesssim t\lesssim 21$ and $\Delta=-1/2$ during $30\lesssim t\lesssim 41$) correspond to the (doubly degenerate) ground states in equilibrium, whereas the remaining one (the state $\Delta=\mp 1/2$ during $21\lesssim t\lesssim 30$) corresponds to neither the ground state nor the transient states appearing in Fig. 1. This new state is metastable with the quasienergy $E_s\approx -1$, and does not carry a voltage. It has no counterpart in equilibrium, and originates from dynamics. (See $\mathscr{E}$ in Fig. 2 for the typical configuration.) Here different initial conditions lead to another new state with the typical configuration given by $\mathscr{F}$ of Fig. 2. Thus on the step $\langle V\rangle=1/3$, there are three (dynamically) accessible states $\mathscr{A}$,$\mathscr{B}$, and $\mathscr{E}$ or $\mathscr{F}$, leading to the time evolution $\{\mathscr{AEB}\}$ or $\{\mathscr{BFA}\}$. In Fig. 3(b), α and γ are shown to be periodic with period $4(2\pi/\omega)$ corresponding to the step $\langle V\rangle=1/4$. This step involves four distinguishable states which are stable and not voltage carrying: While two of them (the states $\Delta=1/2$ during $20\lesssim t\lesssim 31$ and $\Delta=-1/2$ during $40\lesssim t\lesssim 51$) correspond to the ground states, the other two (the states $\Delta=\mp 1/2$ during $31\lesssim t\lesssim 40$ and $\Delta=\pm 1/2$ during $51\lesssim t\lesssim 60$) are new states of dynamic origin, the typical configurations of which are given by $\mathscr{E}$ and $\mathscr{F}$. Thus there exist four accessible states $\mathscr{A}$, $\mathscr{B}$, $\mathscr{E}$, and $\mathscr{F}$; the system evolves with time along $\{\mathscr{AEBF}\}$. We have also considered the steps $\langle V\rangle=1/5$, 1/6, 1/7, and 1/8, which reveal the periods $5(2\pi/\omega)$, $6(2\pi/\omega)$, $7(2\pi/\omega)$, and $8(2\pi/\omega)$, respectively. On these steps, there again appear four states $\mathscr{A}$, $\mathscr{B}$, $\mathscr{E}$, and $\mathscr{F}$. Unlike the system on the step $\langle V\rangle=1/4$, however, the system here visits new states several times in one period, thus effectively increasingthe number of accessible states. The corresponding time evolution is described by $\{\mathscr{BFAEE}\}$, $\{\mathscr{AEEBFF}\}$, $\{\mathscr{EBFFAEE}\}$, and $\{\mathscr{AEEEBFFF}\}$, respectively.

Finally, we consider the time evolution on higher-order subharmonic steps. The behaviors of them are similar to those on higher-order half-integer and integer steps; i.e., the period is $q(2\pi/\omega)$ for $\langle V\rangle=p/q$, and transient states, which are characterized by $\mathscr{C}$ and $\mathscr{D}$ of Fig. 2, are introduced. We have observed that the system evolves with time in one pe-

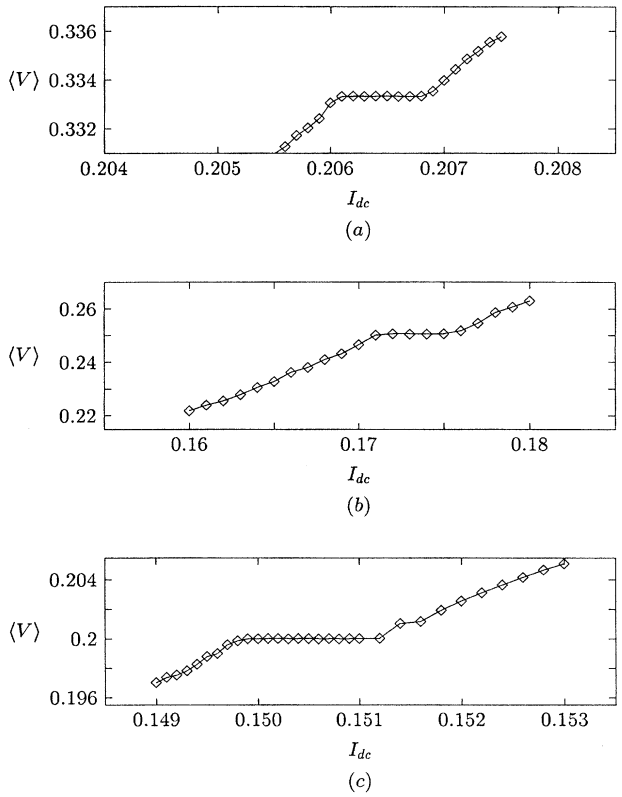

FIG. 4. Simulated IV characteristics at low temperatures for the $N=16$ square array with $f=1/2$, displaying subharmonic steps at (a) $\langle V\rangle=1/3$ at $T=0.01$ (in units of $ek_B/\hbar I_c$), (b) $\langle V\rangle=1/4$ at $T=0.1$, and (c) $\langle V\rangle=1/5$ at $T=0.001$. Lines are merely guides to the eye.

riod according to $\{\mathcal{BDECA}\}$ on the step $\langle V\rangle=2/3$ and $\{\mathcal{DBDFDCAC}\}$ on the step $\langle V\rangle=4/3$, respectively. On the step $\langle V\rangle=2/5$, on the other hand, the time evolution is found to be $\{\mathcal{ABABF}\}$, which does not involve any intervening transient states although it is a higher-order subharmonic step. In general no transient states appear in the time evolution on the step $\langle V\rangle=p/q\leq 1/2$.

These observations together with investigation of other subharmonic steps lead to the following conclusion: On the integer step $\langle V\rangle=p$, the period of the time evolution is still given by $(2\pi/\omega)$ regardless of p. The phase configuration evolves with time according to $\{\mathcal{AC}[\mathcal{DC}]^{p-1}\}$ or $\{\mathcal{BD}[\mathcal{CD}]^{p-1}\}$ in one period, where $[\mathcal{O}]^n$ represents n consecutive repetitions of $\mathcal{O}$. On the half-integer step $\langle V\rangle=p/2$ with an odd integer p, on the other hand, the period is $2(2\pi/\omega)$ while the time evolution of the phase configuration is $\{\mathcal{A}[\mathcal{CD}]^{(p-1)/2}\mathcal{B}[\mathcal{DC}]^{(p-1)/2}\}$. Thus it is concluded that on integer or half-integer steps the numerator p does not change the period; for $p>1$, however, transient states $\mathcal{C}$ and $\mathcal{D}$ are involved in the time evolution. Similar features can also be observed on subharmonic steps: With the four different dynamically accessible states $\mathcal{A}$, $\mathcal{B}$, $\mathcal{E}$, and $\mathcal{F}$, one can construct arrangements of q states for any positive integer q. On the subharmonic step $\langle V\rangle=1/q$, the system evolves along such q-state arrangements consisting of four different dynamical states, with period $q(2\pi/\omega)$.

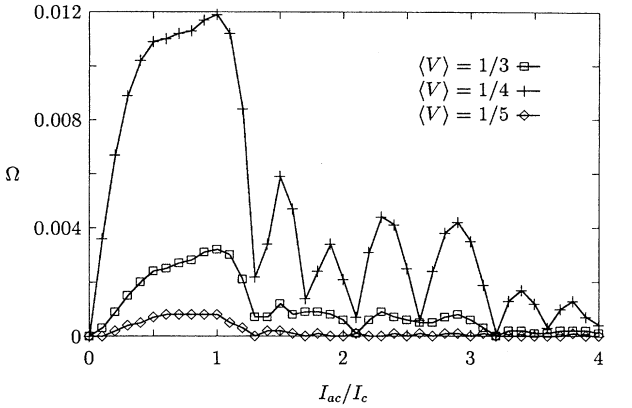

FIG. 5. Widths of the subharmonic steps (□ for $\langle V\rangle=1/3$, + for $\langle V\rangle=1/4$, and ◇ for $\langle V\rangle=1/5$) versus the amplitude of the ac component I_{ac} in a square array with $f=1/2$. Lines are merely guides to the eye.

The time evolution of the phase configuration within one period is described by $\{\mathcal{B}[\mathcal{F}]^{(q-3)/2}\mathcal{A}[\mathcal{E}]^{(q-1)/2}\}$ or $\{\mathcal{B}[\mathcal{F}]^{(q-1)/2}\mathcal{A}[\mathcal{E}]^{(q-3)/2}\}$ for odd q and $\{\mathcal{B}[\mathcal{F}]^{q/2-1}\mathcal{A}[\mathcal{E}]^{q/2-1}\}$ for even q. In general, on steps $\langle V\rangle=p/q$ with relative primes p and q, the time evolution of the phase configuration is also described by q states constructed of four different dynamical states together with voltage-carrying transient states.

The devil's staircase structure obtained from the analysis of Eqs. (7) has been confirmed by numerical simulations.[9] In this paper, the stability against thermal fluctuations has also been studied by numerical simulations at finite temperatures ($T\neq 0$) for system size $N=16$. Figure 4 shows the subharmonic steps are stable against thermal fluctuations if they are sufficiently small. Further, the widths of subharmonic steps for various amplitudes of alternating currents are computed: Figure 5 shows the width Ω of the steps $\langle V\rangle=1/3$, 1/4, and 1/5, which apparently follow the Bessel-function-type behavior, similarly to the case of integer and half-integer steps.[15]

IV. TRIANGULAR ARRAY WITH $f=1/2$

A triangular array is also described by Eq. (6) with the triangular lattice Green's function G_{ij}. The Landau gauge may be chosen such that

$$A_{ij}=\begin{cases}\pm\pi f(4x_i+1) & \text{for } \mathbf{r}_j=\mathbf{r}_i+\hat{\mathbf{x}}/2\pm\sqrt{3}/2\hat{\mathbf{y}},\\ \pm\pi f(4x_i-1) & \text{for } \mathbf{r}_j=\mathbf{r}_i-\hat{\mathbf{x}}/2\pm\sqrt{3}/2\hat{\mathbf{y}},\\ 0 & \text{otherwise.}\end{cases}$$

Using the symmetry of the doubly degenerate ground states, which form 1×1 rhombic vortex superlattices,[13] we reduce Eq. (6) to the two coupled equations

$$\frac{d\chi}{dt}=\frac{1}{3}(\sin 2\chi-\sin\chi\cos\psi),\qquad \frac{d\psi}{dt}=\frac{1}{2}I(t)-\cos\chi\sin\psi, \tag{8}$$

where $\chi\equiv(\alpha+\gamma)/2$ and $\psi\equiv(\alpha-\gamma)/2$ with appropriate gauge-invariant phase differences α, β, and γ. (See Fig. 6.) Equations (8) allow us to calculate the time-averaged voltage

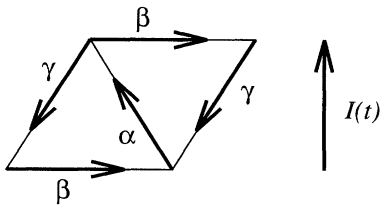

FIG. 6. Gauge-invariant phase differences on a vortex superlattice unit cell of a triangular array with $f=1/2$. The direction of the external current $I(t)$ is also indicated.

$\langle V\rangle$, again giving many subharmonic steps in addition to the standard integer and half-integer steps and eventually producing a devil's staircase structure with self-similarity. Figure 7(a) shows the dynamic resistance $d\langle V\rangle/dI_{\rm dc}$ versus $\langle V\rangle$ for $\omega=\pi/5$ (in units of $2eRI_c/\hbar$) and $I_{\rm ac}=1$ (in units of I_c). The dynamic resistance has many zeros at various rational voltages including $\langle V\rangle=$ 1/12, 1/10, 1/8, 1/6, 1/5, 1/4, 3/10, 1/3, 3/8, 2/5, and 1/2. Calculations with higher precision produces more steps at higher-order rational values of $\langle V\rangle$, eventually revealing a devil's staircase structure. In Figs. 7(b) and 7(c) we show the IV characteristics in two different scales which indeed exhibit self-similarity.

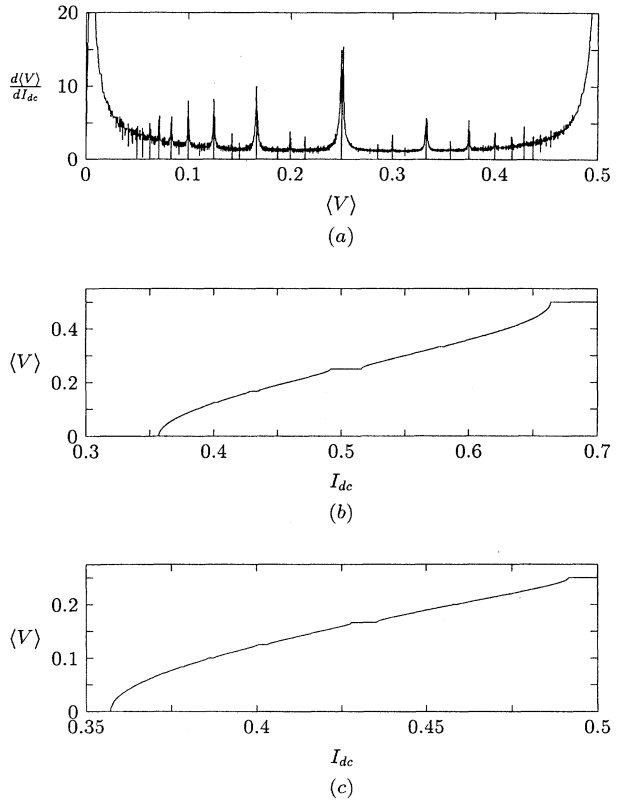

FIG. 7. (a) Dynamic resistance $d\langle V\rangle/dI_{\rm dc}$ (in units of $N\hbar\omega/2e$) versus time-averaged voltage $\langle V\rangle$ in a triangular array with $f=1/2$. The frequency and the amplitude of the ac component are $\omega=\pi/5$ and $I_{\rm ac}=1$, respectively. (b) and (c) show corresponding IV characteristics in different scales. Steps at $\langle V\rangle=1/2$, 1/3, 1/4, 1/6, and 1/8 can be seen in (b) while (c) displays steps at $\langle V\rangle=1/4$, 1/5, 1/6, 1/8, and 1/10.

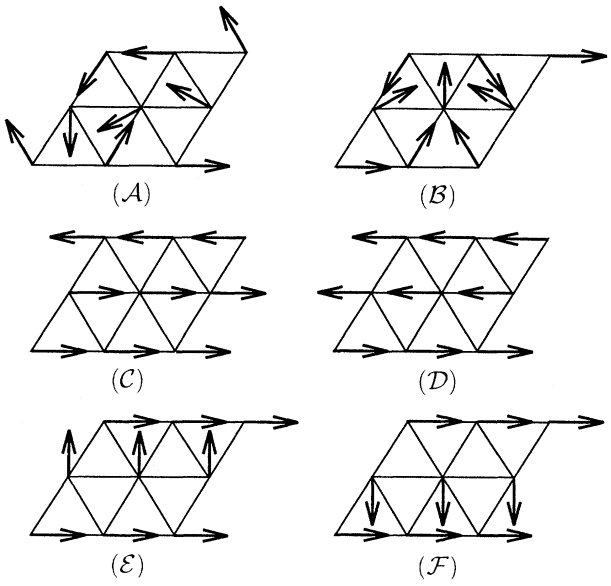

FIG. 8. Typical configurations of the states found in Fig. 9. In each diagram, the position of the center has been chosen as the origin $\mathbf{r}_i=(0,0)$. $\mathscr{A}$ and $\mathscr{B}$ are doubly degenerate ground states in equilibrium, and $\mathscr{C}$ and $\mathscr{D}$ are transient states, while $\mathscr{E}$ and $\mathscr{F}$ are metastable states of dynamical origin. Although the phases are not periodic under translation by the vortex superlattice constant, the gauge-invariant phase differences are periodic.

We study the time evolution of phase differences α and γ, vortex charge $\Delta\equiv(\alpha+\beta+\gamma)/2\pi$, potential difference V, and the quasienergy $E_s\equiv\cos\alpha+\cos\beta+\cos\gamma$ on integer and half-integer steps. Similarly to the fully frustrated square array considered in Sec. III, each state in the time evolution is identified and the period is found to be $2(2\pi/\omega)$ on half-integer steps and $(2\pi/\omega)$ on integer steps. In addition, we have found that the system evolves with time according to $\{\mathscr{A}\mathscr{B}\}$ on the step $\langle V\rangle=1/2$ and $\{\mathscr{B}\mathscr{C}\}$ on the step $\langle V\rangle=1$. On the step $\langle V\rangle=3/2$ and 2, we have also found the time evolution $\{\mathscr{A}\mathscr{D}\mathscr{C}\mathscr{B}\mathscr{C}\mathscr{D}\}$ and $\{\mathscr{B}\mathscr{C}\mathscr{D}\mathscr{C}\}$, respectively. The typical configuration of each state is shown in Fig. 8, where two states $\mathscr{A}$ and $\mathscr{B}$ with vortex charge $\Delta=\pm1/2$, respectively, are simply the doubly degenerate ground states in equilibrium. The other two states $\mathscr{C}$ and $\mathscr{D}$, on the other hand, are voltage-carrying transient states. The above observations allow us to conclude that the time evolution is described by $\mathscr{A}[\mathscr{D}\mathscr{C}]^{(p-1)/2}\mathscr{B}[\mathscr{C}\mathscr{D}]^{(p-1)/2}\}$ on the half-integer step $\langle V\rangle=p/2$, and $\{\mathscr{A}\mathscr{D}[\mathscr{C}\mathscr{D}]^{p-1}\}$ or $\{\mathscr{B}\mathscr{C}[\mathscr{D}\mathscr{C}]^{p-1}\}$ on the integer step $\langle V\rangle=p$.

We next consider subharmonic steps $\langle V\rangle=p/q$ with $q>2$, and show the corresponding evolution in Fig. 9, which reveals that the period is $q(2\pi/\omega)$ irrespective of p. Figure 9 also shows that the system evolves according to (a) $\{\mathscr{A}\mathscr{E}\mathscr{B}\}$ $(2.5\lesssim t\lesssim32.5)$ on the step $\langle V\rangle=1/3$ and (b) $\{\mathscr{A}\mathscr{E}\mathscr{B}\mathscr{F}\}$ $(2\lesssim t\lesssim42)$ on the step $\langle V\rangle=1/4$. On the step $\langle V\rangle=1/5$ and 2/3, we have found the time evolution $\{\mathscr{A}\mathscr{E}\mathscr{E}\mathscr{B}\mathscr{F}\}$ and $\{\mathscr{A}\mathscr{E}\mathscr{F}\mathscr{D}\}$, respectively. The two states $\mathscr{E}$ and $\mathscr{F}$ originate from dynamics, and have typical configurations shown in Fig. 8. In general, there exist two transient states as well as four (meta)stable states, among which two correspond to the doubly degenerate ground states and two

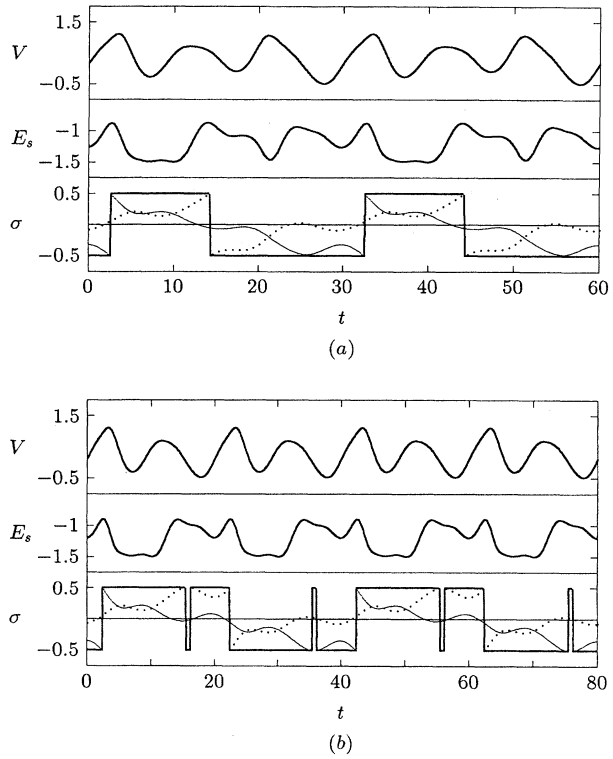

FIG. 9. Time evolution of α, γ, Δ, E_s, and V in a triangular array with $f=1/2$ on subharmonic steps, (a) $\langle V\rangle=1/3$ and (b) $\langle V\rangle=1/4$.

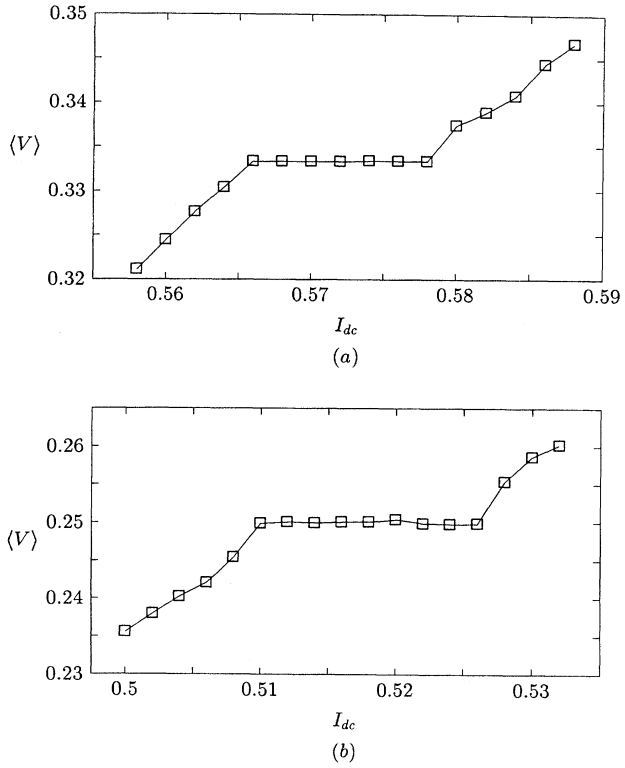

FIG. 10. Simulated IV characteristics for a 12×12 triangular array with $f=1/2$, displaying subharmonic steps at (a) $\langle V\rangle=1/3$ and (b) $\langle V\rangle=1/4$. Lines are merely guides to the eye.

are of dynamical origin. In one period, the system may visit the dynamically generated states many times, thus effectively increasing the number of accessible states. With these four different dynamical states, one can again construct arrangements of q states for any positive integer q: On the subharmonic step $\langle V\rangle=p/q$, the system evolves along such q-state arrangements with period $q(2\pi/\omega)$.

To confirm the subharmonic structure, we have performed numerical simulations of Eq. (6) on a 12×12 triangular array with $f=1/2$, using the method in Ref. 9. Results of simulations are presented in Fig. 10, which displays the subharmonic steps at $\langle V\rangle=$ (a) 1/3 and (b) 1/4. We also calculated widths of subharmonic steps for various amplitudes of the ac component and present them in Fig. 11, which again displays Bessel-function-type behavior.

V. TRIANGULAR ARRAY WITH $f=1/4$

The triangular array with $f=1/4$ is of particular interest with regard to its properties associated with the infinitely degenerate ground states (in the absence of external currents).[13] In the presence of external currents, on the other hand, zero-temperature simulations reveal the symmetry under the 2×2 vortex superlattice translation (see Fig. 12), which allows us to seek the solution of the reduced equations in terms of gauge-invariant phase differences α, β, γ, δ, ε, and ζ:

$$\frac{d\alpha}{dt}=\frac{1}{4}(\sin\varepsilon+\sin\zeta-\sin\gamma-\sin\delta+2\sin\alpha),$$

$$\frac{d\beta}{dt}=\frac{1}{4}(\sin\zeta+\sin\gamma-2\sin\beta-\sin\delta-\sin\varepsilon),$$

$$\frac{d\gamma}{dt}=\frac{1}{4}[2I(t)-\sin\zeta-\sin\delta-2\sin\gamma-\sin\alpha+\sin\beta], \quad (9)$$

with $\zeta=\pi/2+\gamma-\alpha$, $\varepsilon=\beta+\gamma-\alpha-\pi$, and $\delta=\beta+\gamma-\pi/2$. Numerical integration of Eqs. (9) again leads to subharmonic steps as well as the standard integer and fractional steps, and suggests a devil's staircase structure, similarly to

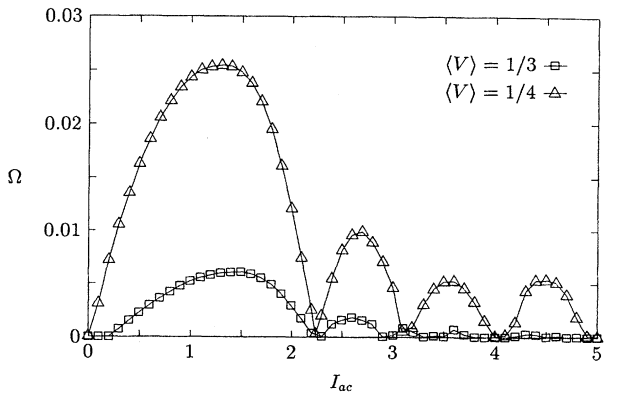

FIG. 11. Widths of the subharmonic steps (□ for $\langle V\rangle=1/3$, and △ for $\langle V\rangle=1/4$) versus the amplitude of the ac component I_{ac} in a triangular array with $f=1/2$. Lines are merely guides to the eye.

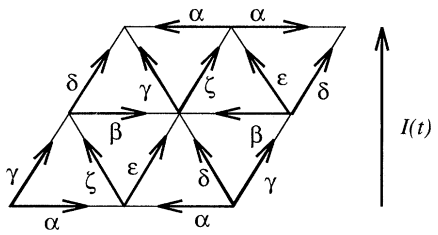

FIG. 12. Gauge-invariant phase differences on a vortex superlattice unit cell of a triangular array with $f=1/4$. The direction of external current $I(t)$ is also indicated.

the case of $f=1/2$. Figure 13 shows the resulting dynamic resistance $d\langle V\rangle/dI_{dc}$ versus $\langle V\rangle$, where zeros of the resistance or steps in the IV characteristic can be observed at various rational voltages including $\langle V\rangle=1/12$, 1/10, 1/8, 1/7, 1/6, 1/5, 1/4, 1/3, 3/8, 2/5, and 1/2.

To study the nature of the subharmonic structure, we again investigate the time evolution of vortex configuration, quasienergy $E_s\equiv-(\cos\alpha+\cos\beta+\cos\gamma+\cos\delta+\cos\varepsilon+\cos\zeta)$, and potential difference V between the top and the bottom of the superlattice unit cell. Since the value of the vortex charge at a particular plaquette cannot classify the vortex configuration of the superlattice, we label the vortex configuration as shown in Fig. 14. Figure 15 displays the time evolution of Δ, E_s, and V on some fractional and integer steps $\langle V\rangle=$ (a) 1/4, (b) 1/2, (c) 1, and (d) 3/4. The period is again given by $q(2\pi/\omega)$ on the step $\langle V\rangle=p/q$. On the step $\langle V\rangle=1/4$ [Fig. 15(a)], the time evolution of the system is characterized by four successive states, each of which can be identified easily with the help of the value of Δ. The quasienergy E_s of these four states are the same as the ground state energy $E_g=-3$, indicating that they originate from the ground states in equilibrium. Figure 15(b) on the step $\langle V\rangle=1/2$ shows that Δ stays with the value 2 and 4 for the most time, taking the value 1 and 3 only momentarily. The states $\Delta=2$ and 4 have the quasienergy $E_s\approx-3$, again suggesting the ground states as their origin. The states $\Delta=1$ and 3, on the other hand, have higher values of the quasienergy and carry voltages, which suggests that they are transient states. Different initial conditions also lead to different time evolution, where the role of the states $\Delta=$ 1 and 3 and that of the states $\Delta=$ 2 and 4 are reversed. Figure 15(c) shows that Δ takes the value 1 for the most time and the values 2, 3, and 4 momentarily. Here the states $\Delta=2$, 3, and 4 have the quasienergy $E_s\approx-2$, corresponding to the transient states.

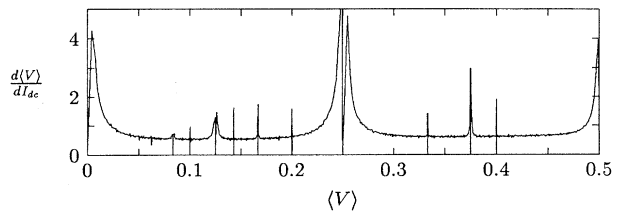

FIG. 13. Dynamic resistance $d\langle V\rangle/dI_{\rm dc}$ (in units of $N\hbar\omega/2e$) versus time-averaged voltage $\langle V\rangle$ in a triangular array with $f=1/4$. The frequency and the amplitude of the ac component are $\omega=\pi/5$ and $I_{\rm ac}=1$, respectively.

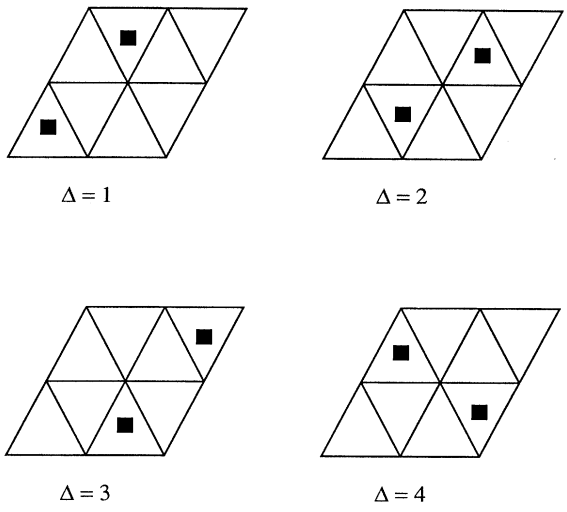

FIG. 14. Vortex configurations labeled by $\Delta=1$, 2, 3, and 4 in a triangular array with $f=1/4$. Solid boxes represent the positions of vortices.

Figure 15(d) describing the step $\langle V\rangle=3/4$ shows that the system evolves with time among eight states: four originating from the ground states and four voltage-carrying transient states. Additional consideration of the higher-order steps suggests the conclusion that on the integer step $\langle V\rangle=p$, the triangular array with $f=1/4$ stays in one state, corresponding to a ground state while the voltage-carrying transient states intervene momentarily. On the half-integer step $\langle V\rangle=p/2$, the system moves from one state to the other (both originating from ground states), between which voltage-carrying transient states intervene. On the fractional step $\langle V\rangle=p/4$, the system moves among the four states, all of which originate from ground states; the voltage-carrying transient states are involved for $p>1$.

Figure 16 shows the time evolution on subharmonic steps $\langle V\rangle=$ (a) 1/3 and (b) 1/6. In Fig. 16(a), there appear four different states: While two of them (the states $\Delta=3$ during $4\lesssim t\lesssim12$ and $\Delta=4$ during $12\lesssim t\lesssim21$) correspond to the ground states in equilibrium with $E_s=-3$, one (the state $\Delta=2$ during $0\lesssim t\lesssim4$) is a transient state carrying a voltage. The remaining one (the state $\Delta=1$ and 2 during $21\lesssim t\lesssim30$) has the quasienergy $E_s\approx-2.8$ and does not carry a voltage; it is a new metastable state of dynamical origin. Thus on the step $\langle V\rangle=1/3$ there appear three dynamically accessible states in addition to one transient state. On the step $\langle V\rangle=1/6$ [Fig. 16(b)], there appear six dynamical states, two of which (the states $\Delta=3$ during $13\lesssim t\lesssim25$ and $\Delta=1$ during $42\lesssim t\lesssim54$) correspond to ground states with the quasienergy $E_s\approx-3$. The remaining four (the states $\Delta=4$ during $25\lesssim t\lesssim35$, $\Delta=4$ during $35\lesssim t\lesssim42$, $\Delta=2$ during $54\lesssim t\lesssim64$, and $\Delta=2$ during $64\lesssim t\lesssim73$) have the quasienergy $E_s\approx-2.8$ which is the same as that of the dynamical state in Fig. 16(a). Thus on the step $\langle V\rangle=1/6$, there exist six accessible states, among which four originate from dynamics. We also find six states originating from dynamics on the step $\langle V\rangle=1/10$, suggesting the existence of many different dynamical states. In general, there appear various metastable states with $E_s>E_g(=-3)$, generated dynami-

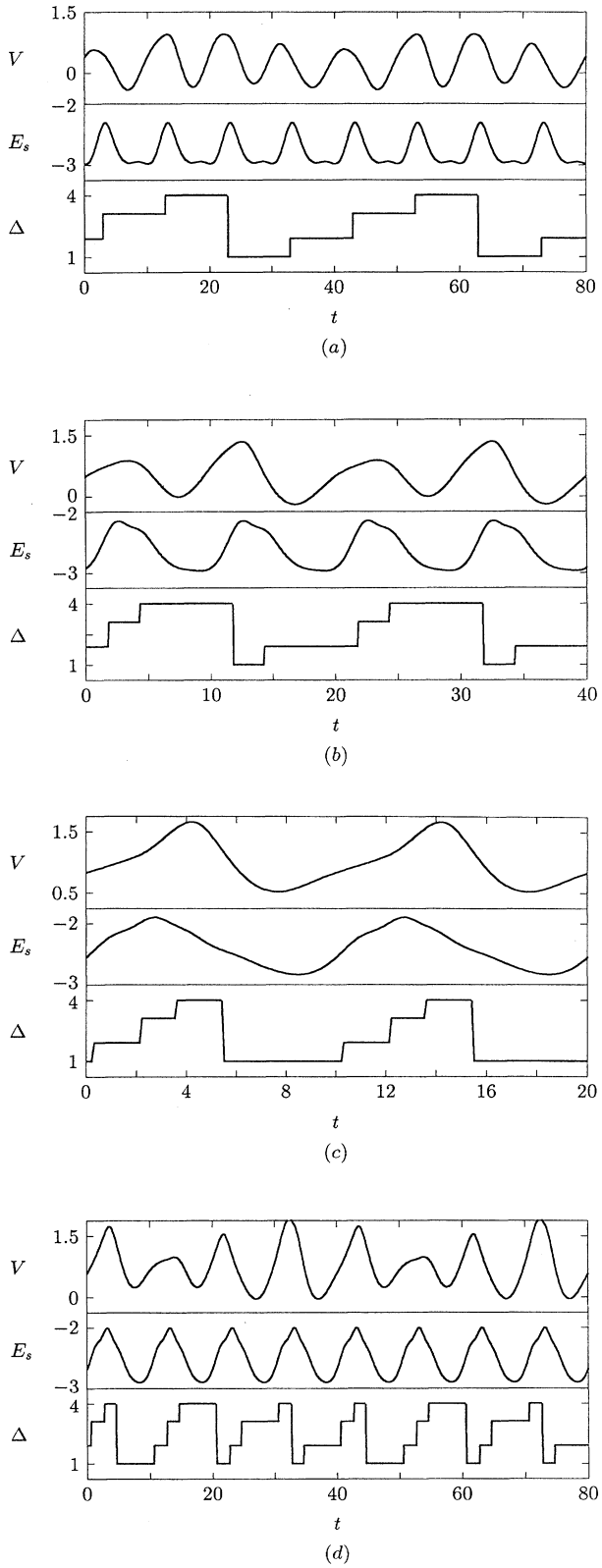

FIG. 15. Stationary-state time evolution of Δ, E_s, and V in a triangular array with $f=1/4$ on fractional and integer steps, (a) $\langle V\rangle=1/4$, (b) $\langle V\rangle=1/2$, (c) $\langle V\rangle=1$, and (d) $\langle V\rangle=3/4$.

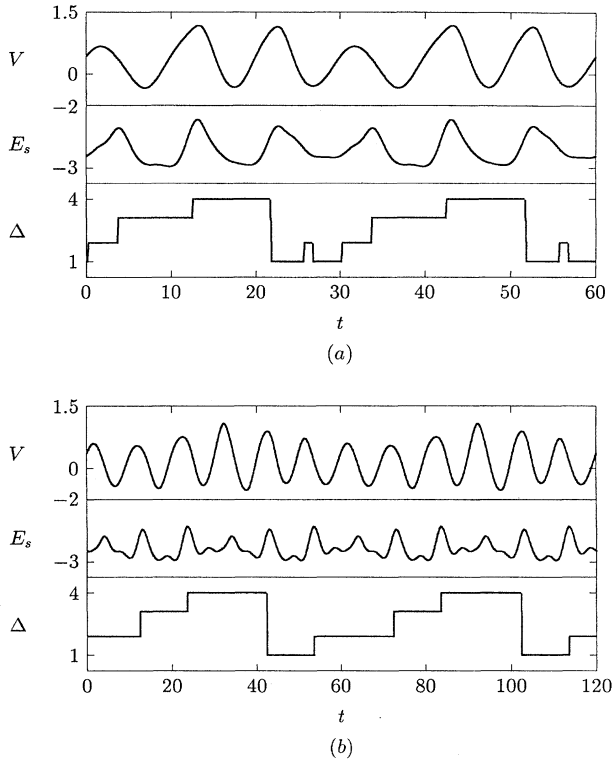

FIG. 16. Time evolution of Δ, E_s, and V in a triangular array with $f=1/4$ on subharmonic steps, (a) $\langle V\rangle=1/3$ and (b) $\langle V\rangle=1/6$.

cally, in addition to the four stable states with $E_s\approx -3$ originating from ground states. The number of the states of the dynamical origin visited by the system is 2, 4, and 6 on the step $\langle V\rangle=1/6$, 1/8, and 1/10, respectively. Thus on the subharmonic step $\langle V\rangle=1/q$, the system evolves, with period $q(2\pi/\omega)$, along the q-state arrangements consisting of q dynamical states, four of which originate from the ground states and the others from dynamics. It is not clear at this stage whether the number of different metastable states visited by the system keeps increasing with q. Unlike the fully frustrated system, there is possibility that it increases indefinitely, reflecting the infinite degeneracy in equilibrium.

Numerical simulations have also been performed on Eq. (6) via the the method as that used in Secs. III and IV, again yielding subharmonic steps. To check the finite-size effects, we have calculated the widths of subharmonic steps for various system sizes, which are shown in Fig. 17. Apparently, the width of either step $\langle V\rangle=$ (a) 1/3 or (b) 1/8 approaches a finite asymptotic value as the system size grows. We have checked the system size up to $N=128$, and obtain the width in perfect agreement with that computed from Eq. (9). We have also calculated widths of subharmonic steps versus the amplitude of alternating currents and obtained Bessel-function-type behavior very similar to Figs. 5 and 11.

VI. CONCLUSION

We have investigated in detail the response of the system to combined direct and alternating applied currents, with emphasis on the possibility of the subharmonic structure. The

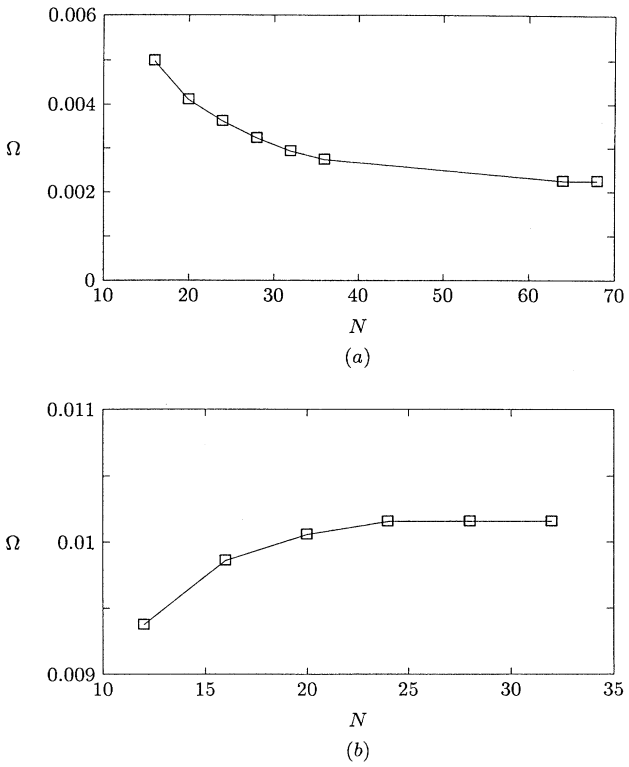

FIG. 17. Widths of the subharmonic steps versus the system size N in a triangular array with $f=1/4$, (a) $\langle V\rangle=1/3$ and (b) $\langle V\rangle=1/8$. Lines are merely guides to the eye.

triangular array with $f=1/4$ as well as fully frustrated square and triangular arrays have been considered. The corresponding equations of motion have been reduced to a few coupled equations through the use of the translational symmetry present in the system. The current-voltage characteristics have been calculated, and shown to exhibit a series of subharmonic steps, suggesting a devil's staircase structure. Such structure is formed out of dynamically accessible states; some of them are generated dynamically while others originate from degenerate ground states in equilibrium. The former are metastable states with the quasienergy higher than that of the latter. Still they are not voltage-carrying states, i.e., $V\approx 0$. In addition to these, there also appear transient states, which possess even higher values of the quasienergy. They are thus unstable and carry nonzero voltages.

On the standard integer and fractional steps, the phase configuration evolves periodically among the stable states originating from the ground states and the voltage-carrying transient states. In contrast, on the subharmonic steps, which cannot be explained in terms of the vortex motion, the states of dynamical origin also play a role: On the step $\langle V\rangle=p/q$, the system evolves, with period $q(2\pi/\omega)$, among q dynamically accessible states together with voltage-carrying transient states. In this case, the number of accessible states is effectively q, and accordingly, the quantization can be explained in terms of topological invariance with the modification that the number of (dynamically) accessible states should be considered instead of the (equilibrium) ground-state degeneracy. These results have been confirmed by extensive simulations, which also show the stability of the subharmonic steps against thermal fluctuations. Finally, the widths of the subharmonic steps have been found to display Bessel-function-type behavior. Since these appear to be general and of wide applicability, we expect the subharmonic structure to be prevalent in arrays with any rational frustration $f=p/q$. It should be stressed that the appearance of the subharmonic structure is closely related to the presence of the frustration in the system. In the unfrustrated system with a nondegenerate ground state [except for those associated with the U(1) symmetry], no additional dynamical states are generated. Thus there is only one accessible state, yielding only the standard integer steps, which has been confirmed by extensive simulations on an unfrustrated array.

ACKNOWLEDGMENTS

This work was supported in part by the SNU-Daewoo Research Fund, by the Basic Science Research Institute Program, Ministry of Education of Korea, and by the Korea Science and Engineering Foundation through the SRC Program.

*Present address: Research Department, Electronics and Telecommunications Research Institute, P.O. Box, 106, Taejon, Korea.

[1] For a list of references, see, e.g., *Proceedings of the 2nd CTP Workshop on Statistical Physics: KT Transition and Superconducting Arrays*, edited by D. Kim, J. S. Chung, and M. Y. Choi (Min Eum Sa, Seoul, 1993).

[2] V. Ambegaokar, B. I. Halperin, D. R. Nelson, and E. D. Siggia, Phys. Rev. B **21**, 1806 (1980); S. Sujani, B. Chattopadhyay, and S. R. Shenoy, *ibid.* **50**, 16 668 (1994).

[3] K. H. Lee, D. Stroud, and J. S. Chung, Phys. Rev. Lett. **64**, 962 (1990); J. U. Free, S. P. Benz, M. S. Rzchowski, M. Tinkham, C. J. Lobb, and M. Octavio, Phys. Rev. B **41**, 7267 (1990); K. H. Lee and D. Stroud, *ibid.* **43**, 5280 (1991).

[4] S. P. Benz, M. S. Rzchowski, M. Tinkham, and C. J. Lobb, Phys. Rev. Lett. **64**, 693 (1990); H. C. Lee, R. S. Newrock, D. B. Mast, S. E. Hebboul, J. C. Garland, and C. J. Lobb, Phys. Rev. B **44**, 921 (1991).

[5] M. Y. Choi, Phys. Rev. B **46**, 564 (1992).

[6] T. C. Halsey, Phys. Rev. B **41**, 11 634 (1990).

[7] L. L. Sohn, M. S. Rzchowski, J. U. Free, S. P. Benz, and M. Tinkham, Phys. Rev. B **44**, 925 (1991).

[8] D. Dominguez and J. V. José, Phys. Rev. Lett. **69**, 514 (1992).

[9] S. Kim and M. Y. Choi, Europhys. Lett. **23**, 217 (1993).

[10] Such subharmonic structure has been also found in small arrays consisting of a few plaquettes. See J. Kim and H. J. Lee, Phys.

Rev. B **47**, 582 (1993); J. Kim, W. G. Choe, S. Kim, and H. J. Lee, *ibid.* **49**, 459 (1994); J. C. Ciria and C. Giovannella (unpublished).
[11] V. Ambegaokar and B. I. Halperin, Phys. Rev. Lett. **22**, 1364 (1969).
[12] S. Kim, M. Y. Choi, and J. S. Chung, J. Phys. A **25**, L1203 (1992); S. Kim and M. Y. Choi, Phys. Rev. B **48**, 322 (1993).
[13] M. Y. Choi and S. Doniach, Phys. Rev. B **31**, 4516 (1985).
[14] S. P. Benz, M. S. Rzchowski, M. Tinkham, and C. J. Lobb, Phys. Rev. B **42**, 6165 (1990).
[15] M. S. Rzchowski, L. L. Sohn, and M. Tinkham, Phys. Rev. B **43**, 8682 (1991).